

Noname manuscript No.
(will be inserted by the editor)

Modelling transition phenomena of scientific coauthorship networks

Zheng Xie · Enming Dong · Zhenzheng
Ouyang · Dongyun Yi · Jianping Li

Received: date / Accepted: date

Abstract In a range of scientific coauthorship networks, transitions emerge in degree distributions, correlations between degrees and local clustering coefficients, etc. The existence of those transitions could be regarded as a result of the diversity in collaboration behaviours of scientific fields. A growing geometric hypergraph built on a cluster of concentric circles is proposed to model two specific collaboration behaviours, namely the behaviour of leaders and that of other members in research teams. The model successfully predicts the transitions, as well as many common features of coauthorship networks. Particularly, it realizes a process of deriving the complex “scale-free” property from the simple “yes/no” decisions. Moreover, it gives a reasonable explanation for the emergence of transitions with the difference of collaboration behaviours between leaders and other members. The difference emerges in the evolution of research teams, which synthetically addresses several specific factors of generating collaborations, namely the communications between research teams, the academic impacts and homophily of authors.

Keywords Coauthorship network · Hypergraph · Geometric graph · Modelling

1 Introduction

Coauthorship networks express collaborations graphically with nodes representing authors, and edges representing coauthor relationships. Since modern sciences increasingly involve collaborative research, the study of coauthorship networks has become an important topic of social science, especially of scientometrics [1]. It helps to understand the evolution and dynamics of scientific activities [2], measure the contributions of scientists [3], predict scientific success [4, 5], etc. The empirically observed coauthorship networks have some

Address(es) of author(s) should be given

common local (degree assortativity, high clustering) and global (power-law degree distribution, short average distance) properties [6–9], according to which they are marked as scale-free and small-world networks. Some important models have been proposed to reproduce those properties, such as modeling the scale-free property by preferential attachment [10–16] or cumulative advantage [17], modeling the degree assortativity by connecting two non-connected nodes, which have similar degrees [18].

One explanation for the power-law tails of degree distributions is the inhomogeneous influences of nodes, which means that nodes with wider influences are likely to gain more connections. A specific example is that authors with large academic impacts, which often occupy a small fraction of the total authors in empirical coauthorship networks, capture voluminous collaborators. When using geometric graph theory (RGG) [19, 20] to analyze networks, such as citation networks, web-graphs, the impacts of nodes in scientific research or Internet can be modeled by attaching specific geometric zones to nodes [21–23]. Likewise the geometric graph model for coauthorship networks [24], which is built on a circle and reproduces the aforementioned features of coauthorship networks at certain levels.

Besides the academic impacts, the homophily of authors in the sense of geographical distances and research interests is another factor of generating collaborations [25, 26]. Comparing with topological graph models, an advantage of the model in Reference [24] is that it models the homophily by spatial coordinates of nodes. However, this model generates all authors at one time, so it cannot express the formation process of coauthorship networks. A growing geometric hypergraph is proposed here to model this process. It is built on a cluster of concentric circles, where each circle has a time coordinate.

The proposed model imitates the collaborations in and between research teams in dynamic ways. The main collaborations occur in the same research team, the mechanism of which synthetically expresses the influences of the homophily and the academic impacts of authors on collaborations in geometrical ways. Our analysis demonstrates that the model can also capture the aforementioned features of the empirical data.

Interesting phenomena of the empirical data are the transitions emerged in degree distributions $P(k)$, average local clustering coefficient and average degree of neighbors as functions of degrees ($C(k)$, $N(k)$). The data features are different in the two regions of k splitted by cross-over regions or tipping points. For example, the $P(k)$ of each empirical data emerges a generalized Poisson and a power-law in small and large k regions respectively, where there exists a cross-over between the two regions. Our model successfully reproduces the shapes of those functions as well as their transitions, and gives reasonable explanations for those transitions.

The components of authors with voluminous collaborators are analyzed. The members of large “paper team”s (each team is a group of authors in a paper) are large degree authors. It is found that when removing large paper teams, the degree distributions still have a power-law tail. Our model provides

a reasonable explanation for the finding: the power-law tails are caused by the papers with many authors as well as the leaders of large research teams.

This report is organized as follows: the model and data are described in Sections 2 and 3 respectively; the degree distribution, clustering and assortativity are analyzed in Sections 4 and 5 respectively; the conclusion is drawn in Section 6.

2 The model

2.1 The model processes

In reality, most researchers belong to research teams in universities and research institutes. For each research team, one or several researchers are responsible for the running of the team as leaders. Research teams and their leaders are the main objects in our model, which have been used in Reference [24]. The term “article team” in Reference [17] is also adopted by our model, which is renamed as “paper team”.

Our model creates “authors” (nodes) by a unit intensity Poisson process on a cluster of concentric circles. The circles could be regarded as “topic” or “interest” spaces. Note that it is not real topic or interest spaces, which are high dimensional spaces representing textual contents of authors’ papers. The model randomly selects some nodes as “leaders” (called lead nodes) to attach specific geometric zones imitating their academic impacts. For each lead node, its “research team” is formed by the nodes within its influential zone (Fig. 1). Unlike the “lead authors” who are in charge of “article teams” in S. Milojević’s model [17], the lead nodes in our model are in charge of “research teams”, and concurrently play the roles of “lead authors” in “article teams”.

Inspired by the processes of generating coauthorship networks, the model generates hypergraphs first (in which nodes are regarded as “authors” and hyperedges as “paper teams”), then extracts simple graphs from the hypergraphs (in which edges are formed between every two nodes in each hyperedge). Note that the isolated nodes are ignored, and the multiple edges are treated as one.

Since new papers are published per week or month, coauthorship networks evolve over time. Our model aims at simulating the evolution processes, especially the self-organizing formation of research teams in the processes. For this purpose, the numbers of hyperedges and nodes in the model are growing over time t . Parameter t can be explained as the t -th unit of time, such as t -th week, t -th month, etc.

The empirical distributions of hyperedge sizes appear a hook head and a fat tail, which can be sufficiently fitted by generalized Poisson and power-law distributions respectively (Fig. 2). Denote the probability density function (PDF) of such distributions by $f(x)$, $x \in \mathbb{Z}^+$. Denote the PDFs of generalized Poisson and power-law by $f_1(x) = a(a + bx)^{x-1} e^{-a-bx} / x!$ and $f_2(x) = cx^{-d}$ respectively, where $a, b, c, d \in \mathbb{R}^+$, and x belongs to some subsets of \mathbb{Z}^+ . We can generate random variables of an $f(x)$ with head $f_1(x)$ and tail $f_2(x)$ by sampling

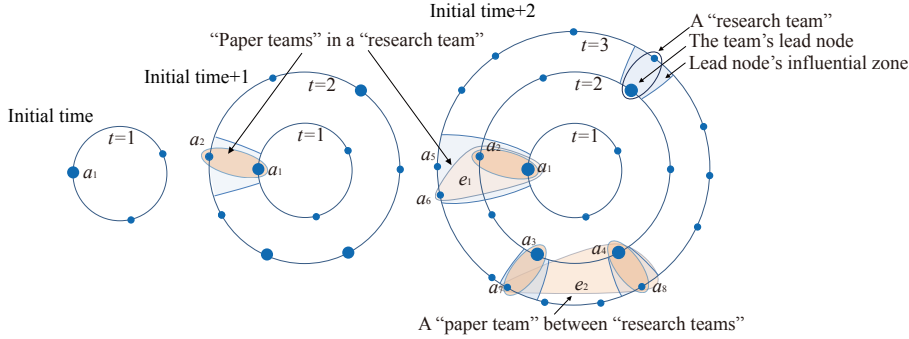


Fig. 1 Illustration of the model. The lead nodes (large nodes) have zones representing their academic impacts, the sizes of which change over time. The set of nodes in a zone (blue area) is regarded as a “research team”, and the set of nodes in a hyperedge (orange area) as a “paper team”. The sizes of “research teams” are in proportion to the corresponding geometric sizes.

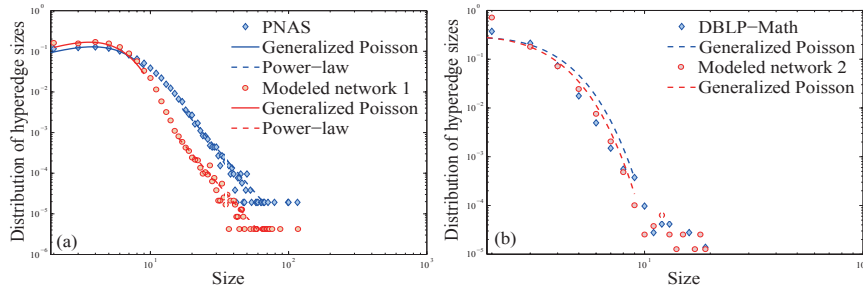


Fig. 2 The distributions of hyperedge sizes. Panels show the distributions of two modeled hypergraphs (parameters of which are listed in Section 3), PNAS 1999-2013 and DBLP-Math 1956-2013 respectively. The root mean squared errors (RMSE, used for measuring the goodness of fit) are 0.015 (generalized Poisson), 0.002 (power-law) for PNAS. 0.015 (generalized Poisson), 0.002 (power-law) for Modeled network 1, 0.113 for DBLP-Math, and 0.113 for Modeled network 2.

random variables of $f_1(x)$ and $f_2(x)$ with probability q and $1 - q$ respectively. In our model, some hyperedge-sizes are drawn from a given $f(x)$.

Based on above preparations, we build a hypergraph on a cluster of concentric circles S_t^1 , $t = 1, 2, \dots, T$ ($T \in \mathbb{Z}^+$) as follows:

1. Coordinate and influential zone (simply ‘zone’ hereafter) assignment

For time $t = 1, 2, \dots, T$ do:

Sprinkle N_1 nodes as “potential authors” uniformly and randomly on a circle S_t^1 . Identify each node, e.g. i , by its spatio-temporal coordinates (θ_i, t_i) , where t_i is the generating time of i ;

Select N_2 nodes from the new nodes randomly as lead nodes to attach specific zones: the zone of a lead node, e.g. j , is defined as an interval of angular coordinate with center θ_j and length $\alpha(\theta_j)t_j^{-\beta}t^{\beta-1}$, where $\alpha(\theta_j)$ is a piecewise constant non-negative function of $\theta_j \in [0, 2\pi)$, and $\beta \in [0.5, 1]$;

2. Connection rules (simply ‘Rule’ hereafter)

For time $t = 1, 2, \dots, T$ do:

- (a) For each new node i , search the existing lead nodes whose zones cover i . For each such lead node j , generate a hyperedge with size m by grouping together i , j and $m - 2$ neighbors of j nearest to i , where m is a random variable drawn from a given $f(x)$ or the number of j ’s neighbors plus two if the former is larger than the latter.
- (b) Select N_3 existing nodes (no distinction is made between lead nodes and the others) with non-zero degree randomly. For each selected node l , generate a hyperedge by grouping together l and $m - 1$ randomly selected nodes with the same degree of l , where m is a random variable drawn from a given $f(x)$ or the number of nodes with the same degree of l if the former is larger than the latter.

Here randomly selecting means sampling without replacement. In reality, most paper teams are subsets of research teams, which are often formed by a leader and some members of the leader’s research team who have similar research interests. This collaboration mode is imitated by Rule (a), which groups together a certain number of nearest nodes and their lead node as a hyperedge. Meanwhile, a few paper teams are unions of some subsets from different research teams, even from different countries [27]. Such teams are very likely to appear in interdisciplinary papers, which account a relatively small fraction of total research papers. For example, the proportion of the papers marked as interdisciplinary ones in PNAS 1999-2013 is 5.7% [28]. The collaborations between research teams are modeled by Rule (b), which gives a possibility to connect the nodes in different research teams. Researchers can join different research teams. This phenomenon also is equivalently imitated by Rule (b) to some extents.

There are some oversimple assumptions in our model. (1) The linear growth of “authors” could not hold in reality. If changing it, the formula of influential zones should be changed to capture features of empirical data. (2) In Rule (b), grouping together certain numbers of nodes with the same degree is the simplest expression of the degree assortativity of authors in empirical data: authors prefer to collaborate with other authors with similar degrees [25]. More reasonable expressions of degree assortativity still need further research.

2.2 Innovation of the model

The improvements in the ability to reproduce empirical features (which will be shown in following sections) are achieved by the new features of the new model, rather than by better selection parameters of the model in Reference [24]. For example, the way of generating hyperedges is different. A new node will “coauthor” with its lead nodes, and some existing nodes in the lead nodes’ zones, which are nearest to it in the sense of space. Therefore, in the end, an older node (which could be non-lead node) can generate hyperedges together with the nodes which are not its nearest neighbors, since the nearest neighbors

may not be generated when the hyperedges were generated. This difference causes the diversity of ages not only for lead nodes (which is addressed by the model in Reference [24]), but also for other nodes. As shown in Fig. 1, when the new node a_6 at time $t = 3$ generates a hyperedge (which contains three nodes), it should “coauthor” with its lead node a_1 and one nearest existing nodes in the zone of a_1 , namely a_2 , but not the nearest one a_5 .

Note that there exists a difference between BA model [10] and our model. In BA model, nodes make decisions to connect existing nodes based on understanding of all nodes’ degrees. In our model, most of the connection decisions made by nodes are restricted by geometric locations, and are local behaviors. Those decisions are imitated by Rule (a). A few decisions are made randomly, which are modelled by Rule (b). In reality, authors making decisions to choose collaborators has the locality of geography and research interests, as well as certain uncertainty or randomness.

The model expresses the sizes of real leaders’ academic impacts and those of their research teams by the sizes of lead nodes’ influential zones. For a lead node i , the size of its “research team” (the number of members in its zone) is $\delta\alpha(\theta_i)t_i^{-\beta}t^{\beta-1}$ at time $t > t_i$, where $\delta = N_1/(2\pi)$. Hence the cumulative number of nodes in the zone is

$$n(\theta_i, t_i, t) = \delta \times \left(\sum_{s=t_i+1}^t \alpha(\theta_i)t_i^{-\beta}s^{\beta-1} \right) \approx \frac{\alpha(\theta_i)\delta}{\beta} \left(\frac{t}{t_i} \right)^\beta. \quad (1)$$

There are some intuitive explanations for Formula 1. Firstly, the value of $t - t_i + 1$ is interpreted as the scientific age of a researcher, namely a researcher spending more time on research would have a larger academic impact and more collaborators as well. Hence it is reasonable to consider the sizes and cumulative sizes of research teams as increasing functions of scientific age, consequently decreasing functions of t_i . Secondly, the cumulative sizes of research teams will increase over t due to the continuously coming collaborators (e.g. tutors may have new students every year). Thirdly, the research team sizes may be different in research fields, so $\alpha(\cdot)$ is introduced to the formula. In addition, academic impacts of a leader, so the increment of cumulative research-team size could be considered to shrink over time ($\partial^2 n(\theta_i, t_i, t)/\partial t^2 < 0$) due to the process of retirements or activity decreases. Unlike papers, the aging of authors appears only for the data with large time span. The authors in PNAS 1999-2013 have no aging phenomenon on average, which will be discussed elsewhere. Hence the major role of the factor $t^{\beta-1}$ in the formula of zonal sizes is to tune the exponent of power-law.

A weakness of our model is that it has a lot of parameters. The $f(k)$ in connection rules tunes the distribution of paper-team sizes. Parameters $\alpha(\cdot)$ and β tunes the distribution of collaborators per author. There is no parameter directly tunes the average local clustering coefficient and average neighbor degree. Hence the respectable model-data fit of those properties presented in Section 5 is impressive to us.

3 The data

3.1 The empirical data

In order to test the universal reproduction ability of the proposed model, we analyze two empirical coauthorship networks from two metadata with different collaboration levels (Table 3). One is DBLP-Math, which is constructed from 72,269 papers published in 54 mathematical journals during 1956–2013. The paper data are obtained from the database DBLP on <http://dblp.uni-trier.de/xml/dblp>. The other one is PNAS, which is constructed from 52,803 papers published in the Proceedings of the National Academy of Sciences (PNAS, <http://www.pnas.org>) during 1999–2013.

In the process of extracting networks from those metadata, authors are identified by their names on their papers (NOP). For example, the author named “Carlo M. Croce” on his paper is represented by the name. It is a reliable way to distinguish authors from one another in most cases. However, it will mistake one author as two if the author changes his/her name in different papers, and two authors as one if they have the same name. Those deficiencies will cause the inaccurate for the empirical networks to express real coauthorships.

In References [7–10, 29, 30], authors are identified by surnames and all initials of authors (SAI, e.g. represent “Carlo M. Croce” by “Croce, CM”). Those references say that the inaccurate caused by SAI does not much affect certain research findings, such as the distribution type of collaborators per author, and that type of papers per author. Reference [31] analyzes the papers in PNAS 2012, and shows the small (large) difference between the distribution of collaborators per author identified by NOP (SAI) and that by a proxy of ground-truth. Based on the result in Reference [31] and the information in Table 1, we choose NOP to identify authors here.

In order to analyze the components of authors with large degrees, Sub-PNAS, a sub-network of PNAS, is extracted from the papers, the numbers of authors in which are less than the boundary point of the generalized Poisson part in the distribution of hyperedge sizes. An algorithm is provided to detect boundary points of PDFs by using some statistical technologies synthetically (Table 2). The inputs are paper-team sizes, $g(\cdot) = \log(\cdot)$ and $h(\cdot) = f_1(\cdot)$. Using $\log(\cdot)$ can rescale the differences between the fitting model and empirical data at different scales, which helps to detect the boundary points at small scales.

3.2 The synthetic data

Two synthetic coauthorship networks are generated to reproduce several properties of the empirical data. In order to make the synthetic networks capture a range of empirical features at certain levels, e.g. degree distributions, we have attempted many times to find following parameters. For Modeled net-

Table 1 Top ten authors identified by SAI and NOP respectively.

PNAS	
Papers	Wang Y 318, Zhang Y 287, Li Y 259, Wang J 247, Zhang J 241, Wang X 239, Chen Y 224, Chen J 222, Liu Y 215, Li J 211.
Collaborators	Wang Y 2115, Zhang Y 1984, Li Y 1779, Wang J 1757, Zhang J 1673, Chen Y 1574, Wang X 1548, Liu Y 1426, Zhang X 1421, Liu J 1420.
Papers	Carlo M. Croce 92, Peter G. Schultz 72, Alan R. Fersht 61, Solomon H. Snyder 61, Irving L. Weissman 59, Richard A. Flavell 59, Eric N. Olson 58, Jan-Ake Gustafsson 56, Paul Greengard 55, Andrew V. Schally 53.
Collaborators	Carlo M. Croce 566, Peter G. Schultz 515, Wei Wang 358, Robert Langer 330, Eric S. Lander 329, Jun Wang 327, Richard A. Flavell 326, Lloyd J. Old 318, Tak W. Mak 311, Bernard Henrissat 310.
DBLP-Math	
Papers	Wang Y 321, Li X 273, Li Y 255, Zhang Y 220, Chen Y 219, Wang J 213, Wang X 211, Zhang H 207, Li H 200, Liu Y 200.
Collaborators	Wang Y 363, Li Y 307, Zhang Y 283, Wang J 278, Chen Y 277, Zhang J 268, Li X 260, Wang X 258, Wang L 255, Liu Y 253.
Papers	Mehdi Dehghan 136, Michael A. Henning 128, Abdul-Majid Wazwaz 128, Lutz Volkmann 115, Ravi P. Agarwal 110, Zsolt Tuza 108, Stevo Stevic 107, H. M. Srivastava 107, David J. Evans 106, Muhammad Aslam Noor 95.
Collaborators	H. M. Srivastava 122, Zsolt Tuza 108, Ravi P. Agarwal 94, David J. Evans 83, Paul Erdős 77, Charles J. Colbourn 76, Michael A. Henning 68, Douglas B. West 67, Noga Alon 63, Sylvain Gravier 62.

Table 2 Boundary point detection algorithm for PDFs.

Input: Observations O_s , $s = 1, \dots, n$, rescaling function $g(\cdot)$, fitting model $h(\cdot)$.
For k from 1 to $\max(O_1, \dots, O_n)$ do:
Fit $h(\cdot)$ to the PDF $h_0(\cdot)$ of $\{O_s, s = 1, \dots, n O_s \leq k\}$ by maximum-likelihood estimation;
Do Kolmogorov-Smirnov (KS) test for two data $g(h(t))$ and $g(h_0(t))$, $t = 1, \dots, k$ with the null hypothesis they coming from the same continuous distribution;
Break if the test rejects the null hypothesis at significance level 5%.
Output: The current k as the boundary point.

work 1 (2), $q = 0.9625$ (0.999) in Rule (a), $q = 1$ (0.999) in Rule (b), $f_1(x)$ is the Poisson distribution with mean 5.5 (2.3), and $f_2(x) \propto x^{-3.7}$, $x \in [10, 150]$ ($[11, 20]$) in Rules (a-b). Set $T = 4,500$ (9,000) and $N_1 = 100$ (15) to make the number of nodes comparable to that of the empirical data in magnitude. Set $N_2 = N_1/5$, $\alpha = 0.19$ (0.2) and $\beta = 0.42$ (0.43) to make the average degree comparable to that of the empirical data. Set $N_3 = 1$ (0.5) to make the generated network have a giant component and the node proportion of the giant component comparable to that of the empirical data.

There are some reasons for choosing such parameters. The collaborator numbers of authors (the degrees of nodes) in the empirical data are not very large. So the value of $\alpha(\cdot)$ should be small, when N_1 is large. In reality, the leaders occupy a small fraction of the total researchers (potential authors), so N_2 is supposed to be far less than N_1 . Meanwhile, the number of paper teams

within a research team is far more than that between research teams, so N_3 is supposed to be small. In practice, N_3 could be a decimal belonging to the interval $[0, 1]$, which means implementing Rule (b) under probability N_3 at each time step.

Since the model is stochastic, we generate 20 networks with the same parameters, and compare their statistical indicators in Table 3. The finding is that the model is robust on those indicators.

Table 3 Specific statistical indicators of the analyzed networks.

Network	NN	NE	GCC	AC	AP	MO	PG	NG
PNAS	201,748	1,225,176	0.881	0.230	5.736	0.884	0.868	4,848
DBLP-Math	68,183	99,116	0.756	0.157	9.256	0.935	0.477	15,492
Modeled network 1	193,655	1,261,131	0.788	0.228	5.957	0.952	0.817	6,230
Modeled network 2	70,921	121,685	0.687	0.095	9.429	0.946	0.606	8,940
Sub-PNAS	200,170	1,158,503	0.881	0.097	5.806	0.882	0.867	4,869

The indicators are the numbers of nodes (NN) and edges (NE), global clustering coefficient (GCC), assortativity coefficient (AC), average shortest path length (AP), modularity (MO, calculated by the Louvain method [32]), the node proportion of the giant component (PG), and the number of components (NG). The values of AP of the first, third and fifth networks are calculated by sampling 15,000 pairs of nodes.

One shortcoming of our model is that in order to make some common features of modelled networks fit those of the empirical data, Modeled network 1's distribution of hyperedge sizes does not fit that of PNAS very well, only captures the features of hook-head and fat-tail.

3.3 Specific features in common

The indicator modularity in Table 3 shows that the same as the empirical networks, the modeled networks have clear communities. The reason is that the nodes in the same “research team” probably belong to the same community due to Rule (a), and the connections between “research teams” are small due to Rule (b). Thus edges within communities are significantly more than those between communities, which results to the clear community structures.

In reality, a leader of a research team often collaborates with all of the team members. Hence the leader acts as a hub in the sub-network of coauthorships restricted in the leader's research team. The communications between research teams make empirical coauthorship networks have a giant component. Hence, the authors evolving in the communications (e.g. visiting scholars or students) also act as hubs in macroscopic scale. Therefore, it is reasonable to regard that bi-level (maybe multilevel) hub structures exist in coauthorship networks.

In the model, due to Rule (a), a lead node also plays the role of hub in the subgraph restricted in its zone, because all of the nodes in the zone connect to the lead node. Due to the randomly selection in Rule (b), the nodes in large zones are preferably connected by the nodes of other zones, which makes the

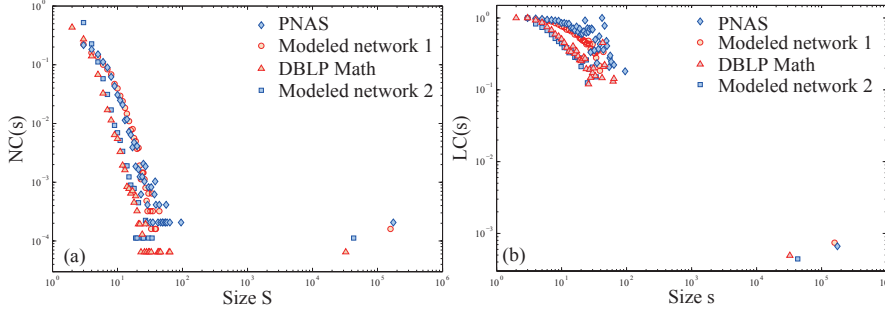


Fig. 3 The distributions of component sizes $NC(s)$ and the average proportion of the largest cliques in s -components (components with size s) $LC(s)$ of the first four networks in Table 3. If there is an s that makes $LC(s) \approx 1$, it means the s -components are nearly fully connected.

nodes in the large zones hubs for the nodes in the small zones. So the modeled networks have a bi-level hub structure. This structure is a reason for that the values of the average shortest path length of the empirical and synthetic networks scale as the logarithms of the number of nodes (Table 3).

Coauthorship networks, in essential, are hypergraphs, which makes the high global clustering coefficient. An author of a paper connecting to the other coauthors generates very many triangles. Together with the small average shortest path length, the synthetic networks can be regarded having the small-world property of the empirical networks.

In the model, a subgraph restricted in a zone will form a component by itself, if its nodes are not selected by Rule (b). The distributions of component sizes are similar to those of the empirical data (Fig. 3a), which validates the reasonability of taking the zonal sizes from a power-law function.

Authors in small research teams (no larger than the mean size of paper teams) are more likely to write papers together. With the growth of research-team-sizes, some authors will stop write, which causes the decreasing trend appearing in the average proportion of the largest cliques in the components with size (Fig. 3b). The model also captures this feature, which reinforces the reasonability of model design.

4 Modeling the transition of degree distributions

4.1 Features of degree distributions

The degree distributions of coauthorship networks (the distributions of collaborators per author) appear two common features, namely a hook head and a fat tail, which can be sufficiently fitted by generalized Poisson and power-law distributions respectively (Fig. 4). The boundary points of generalized Poisson parts in degree distributions are detected by the algorithm in Table 2. Inputs are degrees as observations, $g(\cdot) = \log(\cdot)$ and $h(\cdot) = f_1(\cdot)$.

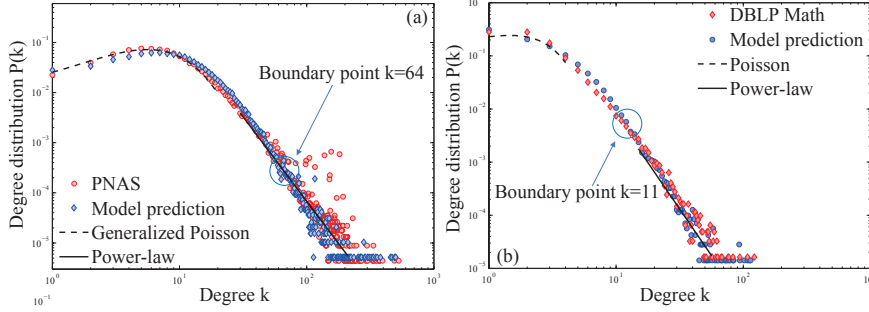


Fig. 4 The degree distributions of the first four networks in Table 3. The fitting functions are the PDFs of generalized Poisson and power-law for the heads and tails respectively. The RMSEs are 0.01 (generalized Poisson), 0.019 (power-law) for PNAS and 0.009 (Poisson), 0.02 (power-law) for DBLP-Math. The fittings pass the KS test at significance level 5%.

In statistics, if regarding authors of a coauthorship network as samples, such a mixture distribution means those samples come from different populations, namely the collaboration mode of authors with small degrees differs from that with large degrees. In reality, the main fraction of the authors are teachers and students in institutes and universities, who can be regarded as two different populations. The collaboration modes of students and teachers are different. Many students only write a few papers, and do not write after graduations, but their teachers could continuously write papers collaborating with their new students or other researchers.

There are two essential questions for the emergence of such degree distributions: Why the distributions emerge generalized Poisson and power-law; Is there any essential relation between them? We attempt to give an answer by analyzing and simulating collaboration modes as follows.

Collaboration behaviors are dependent on authors' choices. We simply treat the choices (e.g. whether or not a researcher joins a research team) as "yes/no" decisions. So the size of a research team is equal to the number of successes in a sequence of n decisions, where n is the number of candidates for the members of the research team. Approximate the probability p of "yes" by its expected value \hat{p} , and suppose those "yes/no" decisions to be independent. Then, the sizes of research teams will follow a binomial distribution $B(n, \hat{p})$. When n is large and \hat{p} is small, $B(n, \hat{p})$ can be approximated by a Poisson distribution with mean $n\hat{p}$ (Poisson limit theorem). The value of $n\hat{p}$ is not a constant due to the diversity of research teams' attractive abilities.

In reality, the "yes/no" decisions could be affected by previous occurrences, e.g. students sometimes introduce their research teams to their juniors. So for small research teams, it is reasonable to regard their sizes as random variables drawn from a range of generalized Poisson distributions (which allow the probability of an event's occurrence to affect by previous events [33]).

For large research teams, the numbers of their candidates are large enough that the "yes/no" decisions can be regarded to be independent. So their sizes

could be regarded as random variables drawn from a range of Poisson distributions with sufficiently large means. The diversity of attractive abilities of research teams gives the possibility of a few research teams having highly attractive abilities, and then guarantees the relative commonness for a few authors getting collaborators that greatly exceed the average. The commonness is a feature of the distribution with a power-law tail, or asymptotically.

4.2 Modelling the features

The analytical derivations (in Appendix) and numerical evidences (the blue diamonds in Fig. 4) illustrate the ability of our model in reproducing the empirical degree distributions. The tunable model parameters give our model flexibility for empirical networks in diverse fields. Specifically, the power exponents of fat tails and the hook peaks can be tuned by β and the expected value of f_1 respectively. In what follows, an intuitionistic explanation is given to show how the geometric aspect of the model is actually necessary to fit the empirical degree distributions.

In our model, nodes are generated according to a Poisson point process, hence the number of nodes covered by a zone is a random variable drawn from a Poisson distribution with an expected value in proportion to the zonal size. Our model generates a range of Poisson distributions with means taking values from a power-law function.

Now we analyze how the emergence of generalized Poisson is captured by our model. The nodes with small degrees usually belong to only one small hyperedge, or come from small “research team”, the sizes of which are no larger than the mean size of hyperedges. For the first case, the empirical data show that the heads of the distributions of hyperedge sizes are well fitted by generalized Poisson (Fig. 2). Hence the degrees of nodes who belong to only one small hyperedge are equal to the size of the hyperedge minus one, hence also follow generalized Poisson distributions. For the second case, nodes in those small “research teams” probably belong to one hyperedge. Ignoring the minority of connections between “research teams” generated by Rule (b), the degrees of those nodes are close to the sizes of corresponding “research teams” minus one, therefore also follow Poisson distributions. Therefore the degrees of authors in small degree region follows a mixture generalized Poisson distribution.

Next we turn to the power-law. The nodes with large degrees are the nodes of large hyperedges or the lead nodes of large research teams. Consider the first case. The tails of the input hyperedge-size distributions follow a power-law distribution, as the empirical data do. For example, in PNAS, the sizes of large hyperedges follow a power-law distribution with exponent $\gamma = -3.96$ (Fig. 2). If supposing each node belongs to only one of such hyperedges, then the degrees of those nodes are drawn from a power-law distribution with exponent $\gamma - 1$. However, the supposition is not fully established in reality (Fig. 5b). Consider the second case. The lead nodes usually “collaborate” with all of their team

members. Ignoring the minority of “collaborations” between “research teams”, the degree of a such lead node is close to the size of its “research team” minus one. A power-law can appear when averaging a range of Poisson distributions with expected values from a power-law function. Our model generates such Poisson distributions by making the sizes of influential zones from a power-law function, which gives a sufficient diversity for lead nodes’ attractive abilities. In fact, the scale-free property of the modelled networks is hidden in the diverse sizes, which is the reason for the respectable data-model fit (Fig. 4).

The mathematical deduction of generating power-law from Poisson is proposed in Appendix, where the calculations in Eq. 4 are inspired by some of the same general ideas as explored in the cosmological networks [20]. In fact, the deduction illustrates the relation between the Poisson and power-law. It shows that “scale-free”, namely the emergence of power-law tails, partly comes from many Poisson processes, consequently from many “yes/no” decisions. In this sense, coauthorship networks give good examples of “1+1>2” for systems science and complexity.

The transition from Poisson to power-law is smooth in DBLP-Math, but nonsmooth in PNAS (Fig. 4). A reason for the difference is that the components of large degree nodes in the two data are different. Authors with large degrees in PNAS partly come from large paper teams (Fig. 5), but DBLP-Math has no large paper team. If an author only writes papers with small paper teams, the growing process of his/her degree is smooth. In our model, this process is represented by the smoothly increasing process of each research team’s cumulative size (Eq. 1). Meanwhile, the model parameter q tunes the proportion of large paper teams. Hence, when q is very small, the transitions of modeled networks, e.g. Modeled network 2, are smooth.

To further show the geometric aspect of the model is actually necessary in fitting the empirical degree distributions, we generate a random hypergraph with the same distribution of hyperedge sizes as that of Modelled network 2. The nodes of each hyperedge are selected randomly. The network has a community structure (MO=0.434), small-world and degree-assortativity properties, but its degree distribution follows a generalized Poisson and has no power-law tail. Therefore, the power-law tails in the modeled distributions of collaborators per author have no direct relation with the corresponding distributions of hyperedge sizes.

5 Modelling the transitions in clustering behaviour and degree correlation

5.1 Transitions in clustering behaviour and degree correlation

As global features, the positive Pearson correlation coefficient (PCC) of degrees between pairs of collaborated authors (degree assortativity) and high global clustering coefficient (GCC, the fraction of connected triples of nodes which also form “triangles”) are common in coauthorship networks. A general

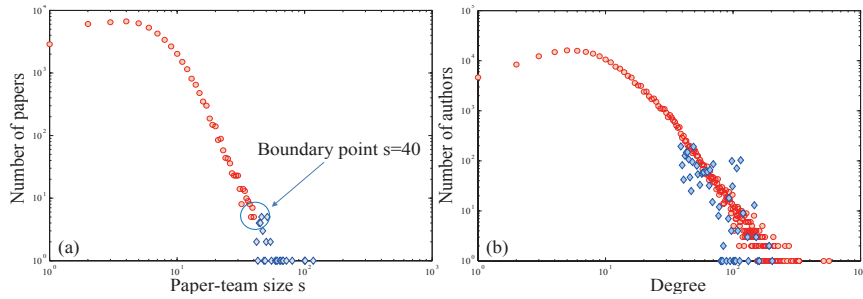


Fig. 5 The components of the authors with many collaborators. Panel (a) shows the distribution of paper-team (hyperedge) sizes and its boundary point (the detecting way of which is described in Section 3) for PNAS 1999-2013. The red circles and blue diamonds in Panel (b) express the degree distributions of the networks extracted from the paper teams with sizes $s < 40$ and $s \geq 40$ respectively.

interpretation for degree assortativity of social networks is the homophily of nodes, namely similar people attract one another [25]. The homophily in research interests is the precondition of collaborations. The homophily is also an explanation for high GCC, because the relation of similarity between nodes is symmetric, reflexive and transitive.

It can be found that the clustering behaviour and degree correlation differ from the authors with small degrees to those with large degrees. Denote the average local clustering coefficient (LCC) and average neighbor degree of k -degree nodes by $C(k)$ and $N(k)$ respectively. Degree correlation can be measured by the slope of $N(k)$ [34]. If the function is increasing, nodes with large degrees connect to nodes with large degrees on average, which means the network is assortative.

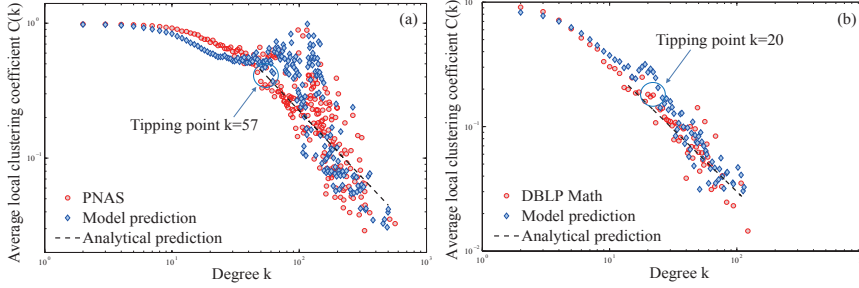
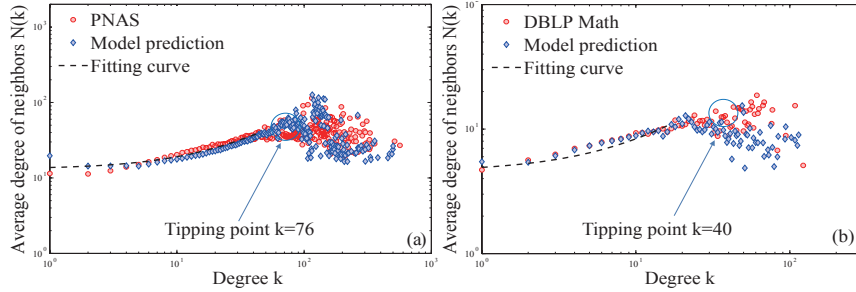
There exist transitions in the $C(k)$ and $N(k)$ of the empirical data (Fig. 6, Fig.7). The tipping points of those functions are detected by the algorithm in Table 4. The inputs are $C(k)/N(k)$, $g(\cdot) = \log(\cdot)$ and $h(s) = a_1 e^{-(s-b_1)/c_1}^2 / h(s) = a_1 x^3 + a_2 x^2 + a_3 x + a_4$. Using the term “tipping point” is suitable for PNAS data, because the features in the two regions splitted by the points have significant difference. However, the term is not quite accurate for the $C(k)$ of DBLP-Math, because its transition is not so sharp. Using boundary point may be more suitable.

When k is larger than the tipping point, the $C(k)$ of each empirical data emerges a decreasing trend, which is proportional to $1/k$. Meanwhile, the PCCs of k and $N(k)$ in the two regions of k splitted by tipping points are $0.416/-0.025$ and $0.250/-0.046$ for PNAS and DBLP-Math respectively. The existence of tipping points in $C(k)$ and $N(k)$ provides an evidence for the difference between the collaboration behaviour of authors with small degrees and that with large degrees.

The low LCCs and non-positive PCC of degree k and $N(k)$ in large k regions cannot be explained by homophily. An explanation is given as follows. The analysis in Section 4 has illustrated that authors in small research teams

Table 4 Boundary point detection algorithm for general functions.

Input: Data vector $h_0(s)$, $s = 1, \dots, K$, rescaling function $g(\cdot)$, fitting model $h(\cdot)$
For k from 1 to K do:
Fit $h(\cdot)$ to $h_0(s)$, $s = 1, \dots, k$ by regression;
Do KS test for two data vectors $g(h(s))$ and $g(h_0(s))$, $s = 1, \dots, k$ with the null hypothesis they coming from the same continuous distribution;
Break if the test rejects the null hypothesis at significance level 5%.
Output: The current k as the boundary point.

**Fig. 6** The relation between local clustering coefficient and degree. The panels show the average local clustering coefficient of k -degree nodes for four networks in Table 3 respectively. The RMSE for the theoretical prediction $C(k) \propto 1/k$ is 0.04597 for PNAS and 0.01476 for DBLP-Math.**Fig. 7** The relation between degree and average degree of neighbors. The panels show k -degree nodes' average degree of their neighbors for four networks in Table 3 respectively. The RMSE for the linearly increasing trend is 3.075 for PNAS and 1.313 for DBLP-Math.

(no larger than the mean size of paper teams) are more likely to write papers together, and have small degrees on average. Hence the authors in a small research team may have high LCCs and similar degrees.

As the cumulative size of a research team increases over time, the degree difference emerges between the leader and the others, because the leader usually collaborates with all members, but non-leaders only write a few papers with a few members on average. So the degrees of non-leaders, on average, do not increase with the growth of their leaders' degrees, which leads to the non-positive PCCs of k and $N(k)$ in large k regions. Meanwhile, the neighbors of non-leaders probably are non-leaders and in the same paper team. So

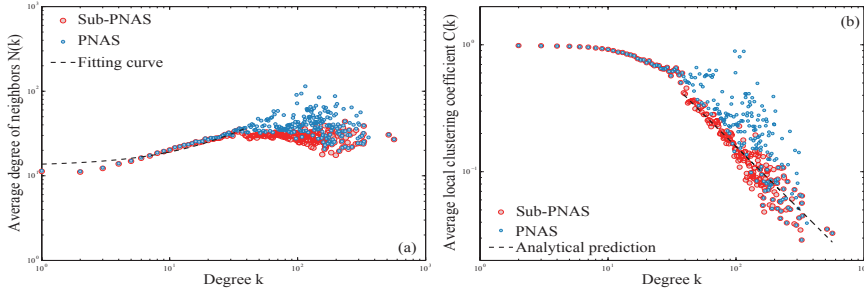


Fig. 8 The influence of large paper teams on local clustering coefficients and average degree of node neighbors. The panels show the average local clustering coefficients and average degree of neighbors for nodes with degree k in Sub-PNAS and PNAS respectively.

non-leaders have high LCCs, and collaborated non-leaders have similar degrees on average, which is a reason for positive PCCs of k and $N(k)$ in small k regions. In the above analysis, the sizes of paper teams are approximated by their expected value. However, the existence of large paper teams can increase the degree correlation coefficients. For example, the PCCs of k and $N(k)$ in the large k -regions are -0.025 and -0.045 for PNAS and Sub-PNAS respectively (Fig. 8a). In addition, some non-leaders could leave their teams, so are unlikely to collaborate with new coming members. For example, many students leave their research teams after graduations, so the students studied in different periods of time are unlikely to collaborate. The leaving also leads to the low LCC of leaders.

5.2 Modelling the transitions

The description in above analysis is imitated by our model. The phenomenon of research-team members leaving and that of members' activity decreasing are imitated by shrinking the influential zones, which makes some existing non-lead nodes no longer be the candidates of the new nodes' "collaborators". Only those non-lead nodes, who are very close to the lead nodes in spacial distances, could receive new "collaborators" persistently. The good model-data fit confirms the reasonability of the model design.

The calculation in Appendix show the tails of $C(k)$ of the modeled networks are proportional to $1/k$, which are similar to those of the empirical networks (Fig. 6). This law is clear in DBLP-Math, but not so clear in PNAS (Fig. 6). The reason is that PNAS has few large paper teams, but the theoretical analysis is based on the mean size of paper teams, and ignores large paper teams (which occur at low-rates). This explanation is confirmed by the clear law in Sub-PNAS, which removes the large paper teams (Fig. 8b).

The model overcomes two fitting defects of the model in Reference [24], namely the $N(k)$ and $C(k)$ of modeled networks are more similar to those of the empirical data. For example, the increasing parts of $N(k)$ here are longer

than those of the result in Reference [24] with the same parameter μ (see Fig. 5 in Reference [24], Fig. 6), a reason of which is described as follows. Suppose node i has an influence zone covers node j . The expected degrees of nodes i and j satisfy $k_i \approx \alpha(\theta_i)\delta t_i^{-\beta}T^\beta/\beta$ and $k_j \leq \mu \log(T/\max(m(\theta_i, t_i), t_j)) + \mu$ respectively. Hence the expected degree of i 's neighbors is larger than that of the model in Reference [24]. This also makes the degree associativity of modeled networks do not require a large μ as the model in Reference [24] does. A small μ makes the $P(k)$ (with a small hook head) and $C(k)$ (with a smooth transition) of Modeled network 2 are all similar to those of DBLP-Math (Fig. 4b, Fig. 6b), and better than those of the model in Reference [24] (see Fig. 4 in Reference [24], Fig. 7).

6 Conclusion

A growing geometric graph is proposed to model coauthorship networks with particular concern on the transition phenomena emerging in special features of those networks. The model overcomes some shortcomings of our previous model, and provides better predictions of some statistical features of the empirical data, e.g. the scaling relation between local clustering coefficient/average degree of neighbors and degree. The model potentially paves a geometric way to understand some aspects of collaboration modes. For example, it explains the emergence of generalized Poisson and power-law in degree distributions by the different collaboration modes of leaders and the other team-members of research teams.

Some shortcomings of the model are indicative of the need for further research: The increment of new nodes should not be fixed; New academic leaders could gain more collaborators than old ones; More reasonable expressions are needed for the academic communications between research teams. We are interested in the transition phenomena in citation networks, which are observed and analyzed by G. J. Peterson et al [35]. Is there any relation between the transition phenomena in citation networks and those in coauthorship networks? Our model is restricted to 1+1-dimensional spacetime. While it is most intuitive and easiest to program, natural variations of the model maybe make sense in high dimensional space, e.g. topic space.

References

1. Glänzel W, Schubert A (2004) Analysing scientific networks through co-authorship. *Handbook of quantitative science and technology research*, 257-276.
2. Mali F, Kronegger L, Doreian P, Ferligoj A, Dynamic scientific coauthorship networks (2012) In: Scharnhorst A, Börner K, Besselaar PVD editors. *Models of science dynamics*. Springer. pp. 195-232.
3. Glänzel W (2014) Analysis of co-authorship patterns at the individual level. *Transinformacao* 26: 229-238.
4. Sarigöl E, Pfitzner R, Scholtes I, Garas A, Schweitzer F (2014) Predicting scientific success based on coauthorship networks. *EPJ Data Science* 3(1): 1-16.

5. Bertsimas D, Brynjolfsson E, Reichman S, Silberholz JM (2014) Moneyball for academics: Network analysis for predicting research impact. Available at SSRN 2374581.
6. Newman M (2001) The structure of scientific collaboration networks. *Proc Natl Acad Sci USA* 98: 404-409.
7. Newman M (2001) Scientific collaboration networks. I. network construction and fundamental results. *Phys Rev E* 64: 016131.
8. Newman M (2001) Scientific collaboration networks. II. shortest paths, weighted networks, and centrality. *Phys Rev E* 64: 016132.
9. Newman M (2004) Coauthorship networks and patterns of scientific collaboration. *Proc Natl Acad Sci USA* 101: 5200-5205.
10. Barabási AL, Jeong H, Néda Z, Ravasz E, Schubert A, Vicsek T. (2002) Evolution of the social network of scientific collaborations. *Physica A* 311: 590-614.
11. Börner K, Maru JT, Goldstone RL (2004) The simultaneous evolution of author and paper networks. *Proc Natl Acad Sci USA* 101(suppl 1), 5266-5273.
12. Moody J (2004) The structure of a social science collaboration network: disciplinary cohesion from 1963 to 1999. *Am Sociol Rev* 69(2): 213-238.
13. Perc C (2010) Growth and structure of Slovenia's scientific collaboration network. *J Informetr* 4: 475-482.
14. Wagner CS, Leydesdorff L (2005) Network structure, self-organization, and the growth of international collaboration in science. *Res Policy* 34(10): 1608-1618.
15. Tomassini M, Luthi L (2007) Empirical analysis of the evolution of a scientific collaboration network. *Physica A* 285: 750-764.
16. Zhou T, Wang BH, Jin YD, He DR, Zhang PP, He Y, et al. (2007) Modeling collaboration networks based on nonlinear preferential attachment. *Int J Mod Phys C* 18: 297-314.
17. Milojević S (2014) Principles of scientific research team formation and evolution. *Proc Natl Acad Sci USA* 111: 3984-3989.
18. Catanzaro M, Caldarelli G, Pietronero L (2004) Assortative model for social networks. *Phys Rev E* 70: 037101.
19. Penrose M, *Random geometric graphs*, Oxford studies in probability, 2003.
20. Krioukov D, Kitsak M, Sinkovits RS, Rideout D, Meyer D, Boguñá M (2012) Network cosmology. *Sci Rep* 2: 793.
21. Xie Z, Ouyang ZZ, Zhang PY, Yi DY, Kong DX (2015) Modeling the citation network by network cosmology. *Plos One* 10(3): e0120687.
22. Xie Z, Ouyang ZZ, Liu Q, Li JP (2016) A geometric graph model for citation networks of exponentially growing scientific papers. *Physica A* 456: 167-175.
23. Xie Z, Rogers T (2016) Scale-invariant geometric random graphs. *Phys Rev E* 93: 032310.
24. Xie Z, Ouyang ZZ, Li JP (2016) A geometric graph model for coauthorship networks. *J Informetr* 10: 299-311.
25. Newman M (2002) Assortative mixing in networks. *Phys Rev Lett* 89: 208701.
26. Hoekman J, Frenken K, Tijssen RJW (2010) Research collaboration at a distance: Changing spatial patterns of scientific collaboration within Europe. *Res Policy* 39: 662-673.
27. Glänzel W (2011) National characteristics in international scientific co-authorship relations. *Scientometrics* 51: 69-115.
28. Xie Z, Duan XJ, Ouyang ZZ, Zhang PY (2015) Quantitative analysis of the interdisciplinarity of applied mathematics. *Plos One* 10(9): e0137424.
29. Liben-Nowell D, Kleinberg J (2007) The link-prediction problem for social networks. *J Am Soc Inf Sci Tec* 58(7), 1019-1031.
30. Milojević S (2010) Modes of Collaboration in Modern Science: Beyond Power Laws and Preferential Attachment. *J Am Soc Inf Sci Tec* 61(7), 1410-1423.
31. Kim J, Diesner J (2016) Distortive effects of initial-based name disambiguation on measurements of large-scale coauthorship networks. *J Am Soc Inf Sci Tec*. 67(6):1446-1461.
32. Blondel VD, Guillaume JL, Lambiotte R, Lefebvre E (2008) Fast unfolding of communities in large networks. *J Stat Mech* 10: P10008.
33. Consul PC, Jain GC (1973) A generalization of the Poisson distribution. *Technometrics* 15(4): 791-799.

34. Pastor-Satorras R, Vzquez A, Vespignani A (2001) Dynamical and correlation properties of the Internet. *Phys Rev Lett* 87(25): 258701.
 35. Peterson GJ, Steve Pressé S, Dill KA (2010) Nonuniversal power law scaling in the probability distribution of scientific citations. *Proc Natl Acad Sci USA* 107: 16023-16027.

7 Appendix

7.1 The underlying formulae of degree distributions

Firstly, we analyze the degree distribution of the network, the edges of which are only generated by Rule (a) in Step 2. The overlapping probability of zones is small, because $\alpha(\cdot)$ is small (due to the limitation of the maximum degree). Hence the overlapping of zones is ignored in the following analysis. We choose a proper q to make the sizes of most hyperedges be drawn from the Poisson part f_1 with mean $\mu + 1$. We initially consider the effect of those hyperedges on the degree distribution, and next consider that of the hyperedges, the sizes of which are drawn from the power-law part f_2 .

Case 1: the degrees of the nodes having zones. Suppose node i has a zone. Let $S(\theta)$ be the smallest s satisfying $n(\theta, s, T) < \mu$. The expected degree of node i contributed by Rule (a) in Step 2 is $k_a(\theta_i, t_i) \approx n(\theta_i, t_i, T)$ and the approximation holds for $t_i \ll T$. If $S(\theta)$ is large enough (which can be achieved by choosing proper parameters) we have a small $|\partial k_a(\theta_i, s)/\partial s|$ for $s > S(\theta)$, and so we take $k_a(\theta_i, s)$ to be independent of s and write $k_a(\theta_i)$ instead of $k_a(\theta_i, t_i)$.

Case 2: the degrees of the nodes having no zone. Assume node i is covered by a zone of node j . If $S(\theta_j) \leq t_j \leq T$, the expected degree of node i contributed by Rule (a) in Step 2, namely by being covered by the zone of j , is $k_a(t_i, \theta_j, t_j) \approx n(\theta_j, t_j, T) \approx k_a(\theta_j) \approx k_a(\theta_i)$, where the third approximation is due to the small distance $d(\theta_i, \theta_j)$ and the piecewise constant property of $\alpha(\cdot)$. Now we suppose $t_j < S(\theta_j)$. Let $m(\theta_j, t_j)$ be the smallest s satisfying $n(\theta_j, t_j, s) > \mu$ and $k_a(t_i, \theta_j, t_j, s)$ be the expected degree of node i at time s . Since the nodes fall randomly and uniformly, the probability of any existing node in the current influential zone of a lead node connecting to a new node is equal. Hence the rate at which node i acquires edges from the nodes coming at time s satisfies

$$\begin{aligned} \partial k_a(t_i, \theta_j, t_j, s)/\partial s &\leq (\mu - 1) \times \alpha(\theta_j) \delta t_j^{-\beta} s^{\beta-1} \times n(\theta_j, t_j, s-1)^{-1} \\ &\approx \beta(\mu - 1)/s. \end{aligned} \quad (2)$$

Therefore $k_a(t_i, \theta_j, t_j) \leq \beta(\mu - 1) \log(T/\max(m(\theta_j, t_j), t_i)) + \mu$. If t_i is large enough, $k_a(t_i, \theta_j, t_j) \approx \mu$. In addition, $k_a(t_i, \theta_j, t_j) < \beta(\mu - 1) \log(T) + \mu$ so can not effect the tail of the degree distribution.

The degrees of nodes will not be exactly equal to their expected values because the nodes are distributed according to a Poisson point process, and so need to be averaged with the Poisson distribution. In addition, the nodes of

the hyperedges with large sizes drawn from f_2 would not have small degrees. Hence the degree distribution of small degree nodes is

$$P_S(k) = \frac{1}{2\pi} \int_0^{2\pi} \left(\frac{\epsilon(\theta) k_a(\theta)^k e^{-k_a(\theta)}}{k!} + \frac{1 - \epsilon(\theta)}{S(\theta) - 1} \sum_{t=1}^{S(\theta)-1} \left(\frac{1}{T - m(\theta, t) + 1} \right. \right. \\ \times \left. \sum_{s=m(\theta, t)}^T \frac{k_a(s, \theta, t)^k e^{-k_a(s, \theta, t)}}{k!} \right) \right) d\theta, \quad (3)$$

where $\epsilon(\theta)$ is the proportion of the nodes covered by the zones of the nodes born on or after time $S(\theta)$. Eq. 3 is a mixture of some Poisson distributions with different expected values, namely the expected degree in small k regain is not a constant. Meanwhile, the probability of adding a new neighbor for a given node is affected by the spacial locations of previous lead nodes. Therefore, it is also reasonable to consider that the predominant modeled collaborations are governed by certain generalization of Poisson processes.

The calculation for the degree distribution in large k region is the same as that in Reference [24], and so is briefly listed as follows:

$$P_L(k) = \frac{1}{2\pi k!} \int_0^{2\pi} \left(\frac{1}{S(\theta)} \int_1^{S(\theta)+1} k_a(\theta, t, T)^k e^{-k_a(\theta, t, T)} dt \right) d\theta \propto \frac{1}{k^{1+\frac{1}{\beta}}}, \quad (4)$$

where $k \gg 0$ is needed in the calculation.

The hyperedges with large sizes drawn from f_2 can affect the tail of degree distribution. Ignoring the overlapping of those hyperedges (which is due to the small probability of their occurrences) and the proportion of the nodes having zones and belonging to those hyperedges (which is small when compared with that of the nodes having no zone) we obtain that the degree distribution's tail of the network generated by Rule (a) in Step 2 is approximately a mixture power-law distribution $qP_L(k) + (1-q)(k+1)f_2(k+1)/\sum_s sf_2(s)$.

Finally, we analyze the degrees contributed by Rule (b). Let $k_b(\theta_i, t_i, s)$ be the degree of node i contributed by this rule at time $s \geq t_i$. The number of nodes with nonzero degree at time s is $N(s) = \zeta \int_0^{2\pi} (\sum_{t=1}^s \alpha(\theta) \delta t^{-\beta} s^\beta / \beta) d\theta \approx s\delta\zeta \int_0^{2\pi} \alpha(\theta) d\theta / (\beta(1-\beta))$, where $\zeta = N_2/(2\pi)$. So the probability that a node is chosen by Rule (b) of Step 2 at time s is $(\nu+1)N_3/N(s)$, where $\nu+1$ is the expected value of f in Rule (b) in Step 2. Hence, the rate at which node i at time s acquires edges generated by Rule (b) is $\partial k_b(t_i, s) / \partial s = \nu(\nu+1)N_3/N(s)$, which gives $k_b(t_i, T) \approx \beta(1-\beta)\nu(\nu+1) \log(T/t_i)N_3 / (\delta\zeta \int_0^{2\pi} \alpha(\theta) d\theta)$. Hence, choosing proper parameters, the degrees contributed by Rule (b) can be ignored, when compared with that contributed by Rule (a) in Step 2.

In simulations, the condition $k \gg 0$ required in Eq. 4 can not be fully satisfied due to the restriction of the maximum degree, which is a reason for the difference between the theoretical value and the practical value of the power exponent. However, the degree distributions of the modeled networks fit the above analysis at certain levels, and are similar to those of the empirical networks respectively (Fig. 4).

7.2 The underlying formulae of the correlation of local clustering coefficients and degrees

Suppose node i has a zone and t_i is small enough. So the number of neighbors of node i generated by Rule (b) in Step 2 can be ignored compared with that generated by Rule (a). Hence the expected degree k of i is approximately equal to $k_a(\theta_i, t_i, T)$. Suppose nodes j, l belong to the zone and $t_j < t_l$. Since t_i is small, k is large, so $T - m(\theta_i, t_i) \approx T - T(\mu/k)^{1/\beta} \approx T$, where $m(\theta_i, t_i)$ is the smallest s satisfying $n(\theta_i, t_i, s) > \mu$. So we can only consider the case $t_j > m(\theta_i, t_i)$. Since the nodes are dropped randomly and uniformly, the probability of an edge between j and l is $\omega T^\beta / (k(t_l - 1)^\beta)$ the reciprocal of the number of nodes (born before t_l) of the zone multiplied by ω , the expected hyperedge size less than two, where the boundary effects of zones are ignored. Averaging over possible values of t_j and t_l , the LCC of node i is

$$\begin{aligned} C(k) &= \frac{1}{T - m(\theta_i, t_i)} \int_{m(\theta_i, t_i)}^T \left(\frac{1}{T - t_j - 1} \int_{t_j+1}^T \frac{\omega T^\beta}{k(t_l - 1)^\beta} dt_l \right) dt_j \\ &\approx \frac{\omega T^{\beta-1}}{k(1-\beta)} \left(\int_{m(\theta_i, t_i)}^T \frac{(T-1)^{1-\beta} - s^{1-\beta}}{T-s-1} ds \right), \end{aligned} \quad (5)$$

where the approximation holds for $T \gg m(\theta_i, t_i)$. Denote the coefficient of $1/k$ by $I(k)$, substitute $m(\theta_i, t_i) \approx T(\mu/k)^{1/\beta}$ into it, and differentiate it to obtain

$$\frac{dI(k)}{dk} = \frac{\omega T^{\beta-1}}{1-\beta} \times \frac{(T-1)^{1-\beta} - T^{1-\beta} \left(\frac{\mu}{k}\right)^{\frac{1-\beta}{\beta}}}{T - T \left(\frac{\mu}{k}\right)^{\frac{1}{\beta}} - 1} \times \frac{T}{\beta} \frac{\mu^{\frac{1}{\beta}}}{k^{\frac{1}{\beta}+1}} \approx \frac{\omega \mu^{\frac{1}{\beta}}}{\beta(1-\beta)k^{\frac{1}{\beta}+1}}, \quad (6)$$

which is approximately equal to 0 if $k \gg \mu$. Hence $I(k)$ is free of k and $C(k) \propto 1/k$ if k is large enough. The modeled networks roughly follow the above analyses (Blue diamonds in Fig. 6), in which the outliers are partly caused by the boundary effects of zones that can not be ignored under the occurrence of some large size hyperedges drawn from $f_2(x)$.